Electron-impact excitation of Li II: A model study of wave-function and collisional approximations and of resonance effects

Randy B. Christensen* and David W. Norcross†
Joint Institute for Laboratory Astrophysics, University of Colorado and National Bureau of Standards, Boulder, Colorado 80309
(Received 13 July 1984)

Results are presented of five-state close-coupling and distorted-wave calculations for electron-impact excitation of Li II from the ground state to the four $n=2$ states ($2\,^3S$, $2\,^1S$, $2\,^3P^o$, $2\,^1P^o$) for energies below the ionization threshold. Sensitivity of the results to scattering approximation, target wave functions, and resonance effects is examined. The spin-allowed transitions are found to be much *more* sensitive to scattering approximation and to the choice of target wave functions than are the spin-forbidden transitions. Resonances contribute noticeably to both spin-allowed and spin-forbidden transitions, but rather more strongly to the latter. Good quantitative agreement is obtained with measurements of the $1\,^1S \rightarrow 2\,^3P^o$ cross section, and of the positions of the lowest $1s\,3l\,3l'$ resonances.

I. INTRODUCTION

Heliumlike ions play important roles in both laboratory and astrophysical plasmas. Since little experimental data are available for the electron-impact excitation cross sections required to determine the strengths of emission lines, calculations must be used. As pointed out by Henry,[1] to limit to 40% the errors in spectroscopically determined impurity densities in fusion plasmas requires that the relevant collision cross sections be known to an accuracy of at least 20%.

The major sources of error in calculations of electron-impact excitation cross sections are inaccuracies in target state wave functions, inadequate treatment of the collision dynamics, and the neglect of resonance effects. At the present time it is not possible to make an *a priori* assessment for heliumlike ions of the relative errors introduced into calculated cross sections from any of the factors just cited. (For an excellent review of this situation, and of e^--ion scattering in general, see Henry[1].) In general, however, calculated cross sections are expected to be most sensitive to inadequacies in the target wave functions, to the treatment of the collision dynamics, and to resonance effects, at near-threshold collision energies in the more weakly ionized members of the isoelectronic sequence.

We present here the results of several sets of calculations for electron-impact excitation of the heliumlike ion Li II to the four $n=2$ excited states (2^3S, 2^1S, 2^3P^o, 2^1P^o). Our main interest is the energy region below the ionization threshold (about 1.2 times the excitation thresholds). The calculations differ as to the quality and type of target wave functions, the collisional approximations, and whether or not resonance effects are included. By comparing the results of the various calculations with each other and with previous work, we hope to learn more about the effects of the possible sources of error.

Li II was chosen because by the criteria mentioned above it should pose a stringent test for theoretical methods, and because the experimental results obtained by Rogers *et al.*[2] for the $1^1S \rightarrow 2^3P^o$ transition can serve as a benchmark by which the absolute accuracy of the calculations can be ascertained. This measurement is particularly interesting as it is the only one to date for a positive ion that involves a change of spin. Pronounced structure was also observed in the near-threshold region, presumably due to unresolved resonances in series converging on the $n=3$ levels. This provides an opportunity for testing an unusual[3,4] technique for including the effect of resonances in scattering calculations, i.e., via correlation functions rather than via additional closed channels in a close-coupling expansion.

II. THEORY AND METHODS

A. Scattering approximations

In our calculations we use the distorted-wave (DW) and close-coupling (CC) approximations in the forms presented by Eissner and Seaton.[5] The CC code IMPACT has been described in detail by Crees *et al.*[6] We present here only an outline of these approximations, emphasizing those aspects that are especially relevant to our calculations. In both approximations the following form for the wave function of the electron plus target system is adopted, for an overall collision symmetry S,L,π:

$$\Psi^{SL\pi} = \sum_{i=1}^{N_{\rm CHF}} \Theta_i^{SL\pi} + \sum_{j=1}^{N_{\rm CHB}} c_j \Phi_j^{SL\pi} . \quad (1)$$

The first summation runs over the $N_{\rm CHF}$ "free-channel" wave functions $\Theta_i^{SL\pi}$, where

$$\Theta_i^{SL\pi} = A\{\theta_i(S_iL_i)F_i(r,\epsilon_i,l)\}^{SL\pi} . \quad (2)$$

The $\theta_i(S_iL_i)$ are the wave functions, usually of configuration-interaction (CI) type, of the target states. The $F_i(r,\epsilon_i,l)$ are the free-electron radial wave functions, and A is the antisymmetrization operator (angular coupling is omitted for compactness). The second summation runs over the $N_{\rm CHB}$ "bound-channel" wave functions $\Phi_j^{SL\pi}$. These may be expressed as

TABLE I. Target wave functions: source of polarized-core orbitals.

$P_\alpha(0)$	α	$P_\alpha(1)$	α	$P_\alpha(2)$	α
$2\bar{s}$	$1s,\ 1^1S$	$3\bar{p}$	$2\bar{p},\ 1^1S$	$3\bar{d}$	$1s,\ 3^3D$
$3\bar{s}$	$1s,\ 2^1S$	$4\bar{p}$	$1s,\ 2^3P^o$		
$4\bar{s}$	$1s,\ 3^3S$	$5\bar{p}$	$1s,\ 3^3P^o$		

$$\Phi_j^{SL\pi}=A\{\phi_j(S_jL_j)P_\alpha(l)\}^{SL\pi}\ , \tag{3}$$

where the $\phi_j(S_jL_j)$ are the single-configuration wave functions used in constructing the CI wave functions $\theta_j(S_jL_j)$, and the $P_\alpha(l)$ are the one-electron radial orbitals used to form the $\phi_j(S_jL_j)$. These $\Phi_j^{SL\pi}$ thus have the form of bound states of the e^-+ion system.

The summation over the $\Phi_j^{SL\pi}$ must be included for completeness in (1) because of the imposition of the orthogonality conditions

$$\langle P_\alpha(l)\,|\,F_i(r,\epsilon_i,l)\rangle=0\ . \tag{4}$$

Notice, however, that the $\Phi_j^{SL\pi}$ are coupled products of the $P_\alpha(l)$ with individual $\phi_j(S_jL_j)$ rather than of the $P_\alpha(l)$ with the total target state wave functions $\theta_j(S_jL_j)$. This allows the bound-channel part of the wave function (1) to represent short-range correlation effects and physically meaningful bound states of the e^-+ion system as well as to compensate for the orthogonality condition.

B. Target state wave functions

In practice, exact wave functions are unavailable for nonhydrogenic targets. Clearly, accurate collision strengths require the use of high-quality target wave functions. The question then arises, "What is a high-quality wave function?" In order to help resolve this question, at least as it applies to Li II, we employ three different CI-type wave functions in our calculations. These models of the target differ both in the nature of the one-electron radial orbitals used and in the configurations included in the CI expansion.

Targets 1 and 2 utilize one-electron radial orbitals generated in polarized-core (PC) calculations[7] for the 1^1S, 2^1S, 2^3P^o, 3^3S, 3^3P^o, and 3^3D bound states of Li II using IMPACT. In the PC calculations the total wave function $\Psi_i^{SL\pi}$ for the Li II target states takes the form

TABLE II. Target wave functions: configuration list.

Target	$1^1S,\ 2^3S,\ 2^1S$
1	$c_1 1s^2+c_2 1s\,2\bar{s}+c_3 1s\,3\bar{s}+c_4 2\bar{p}^{\,2}+c_5 2\bar{p}\,3\bar{p}$
2	target $1+c_6 1s\,4\bar{s}+c_7 3\bar{d}^{\,2}$
3	$c_1 1s^2+c_2 2s^2+c_3 2p^2+c_4 1s\,2s+c_5 1s\,3s+c_6 3d^2$
vW[a]	$c_1 1s^2+c_2 2s^2+c_3 2p^2+c_4 1s\,2s$
	$2^3P^o,\ 2^1P^o$
1	$c_1 1s\,2\bar{p}+c_2 1s\,3\bar{p}+c_3 1s\,4\bar{p}$
2	target $1+c_4 1s\,5\bar{p}+c_5 2\bar{p}\,3\bar{d}$
3	$c_1 1s\,2p+c_2 2s\,2p+c_3 1s\,3p+c_4 2p\,3d$
vW[a]	$c_1 1s\,2p+c_2 2s\,2p$

[a]Reference 9.

$$\Psi_i^{SL\pi}=A\left[1sP_{1s,i}(L)+\sum_{l'=L\pm1}2\bar{p}P_{2\bar{p},i}(l')\right]+\sum_{j=1}^{N_{\rm CHB}}c_j\Phi_j^{SL\pi}\ , \tag{5}$$

where $1s$ is the hydrogenic orbital for Li III and $2\bar{p}$ is the p-type pseudo-orbital that is the first-order perturbation theory correction to the Li III ^2S ground-state wave function in a constant electric field.

Not all of the orbitals generated in the Li II PC calculations are used in targets 1 and 2. Target 1 was determined by testing various sets of configurations, using orbitals from the 1^1S, 2^3S, 2^1S, 2^3P^o, and 2^1P^o PC calculations, until a CI basis set that was reasonably compact yet which gave good energy levels and oscillator strengths was obtained. The result utilizes no orbitals from the 2^3S and 2^1P^o PC calculations. Since no $n=3$ type orbitals are used in target 1, no bound-channel configurations corresponding to autoionizing states of Li I in series converging on the $n=3$ states of Li II are generated in the associated total scattering wave function (1).

Target 2 is a superset of target 1 obtained by including configurations containing orbitals from the 3^3S, 3^3P^o, and 3^3D PC calculations. These configurations were added not with the intent of appreciably increasing wave-function quality, but rather to generate bound-channel configurations of the type $1s\,3l3l'$ in the associated total wave function (1). The orbitals and configurations used in targets 1 and 2 are given in Tables I and II.

The advantages of targets 1 and 2 are that they are simultaneously optimized on both the ground state and the excited states, and that they capture a significant fraction ($\sim$57%) of the ground-state correlation energy. Their major disadvantage is that since they include non-spectroscopic orbitals, some of the eigenvalues of the target Hamiltonian correspond to nonphysical states, usually lying well above the ionization limit. The corresponding bound-channel configuration set can give rise to nonphysical resonance behavior in the calculated R matrices.

The orbitals and configurations in target 3 were selected in a manner similar to that used by Pradhan *et al.*[4] for other members of the helium isoelectronic sequence. The one-electron radial orbitals were generated in a scaled Thomas-Fermi-Dirac (TFD) potential,[8] with the scaling factor λ_0 ($=0.981$) chosen to minimize the ground-state energy and λ_1 ($=0.482$) selected to best reproduce the experimental 2^1S-2^3P^o and 2^3P^o-2^1P^o splittings. The d-type scale factor was set equal to the p-type scale factor. (Tests showed that our results are insensitive to the exact value of the d-type scale factor.) The configurations in target 3 are also given in Table II. Like target 2, target 3 will generate bound-channel configurations of the type $1s\,3l3l'$ in the total scattering wave function (1).

TABLE III. Target wave functions: configuration mixing coefficients.

Target	c_1	c_2	c_3	c_4	c_5	c_6	c_7
				1^1S			
1	0.9838	−0.1744	0.0000	0.0350	0.0238		
2	0.9838	−0.1744	0.0000	0.0350	0.0238	0.0000	0.0001
3	0.9999	−0.0083	0.0064	−0.0063	−0.0022	0.0000	
vW[a]	−0.9999	0.0089	0.0068	0.0021			
				2^3S			
1		−0.6051	0.7961		0.0093		
2		−0.6256	0.7761		0.0097	−0.0789	
3				0.9983	0.0585		
vW[a]				1.0000			
				2^1S			
1	−0.0922	−0.5198	0.8491	0.0092	−0.0135		
2	−0.0922	−0.5197	0.8492	0.0092	−0.0135	0.0004	0.0003
3	0.0069	0.0815	−0.0125	0.9938	−0.0740	0.0001	
vW[a]	0.0029	0.0884	0.0137	0.9960			
				2^3P^o			
1	−0.6576	−0.3939	0.6422				
2	0.6569	0.3935	−0.6431	0.0030	0.0051		
3	0.9975	0.0529	0.0469	0.0026			
vW[a]	0.9983	0.0578					
				2^1P^o			
1	−0.6008	−0.4137	0.6840				
2	0.5908	0.4069	−0.6954	0.0418	−0.0062		
3	0.9975	0.0648	−0.0276	−0.0033			
vW[a]	0.9975	0.0704					

[a]Reference 9.

The advantages of target 3 are that it is simple to obtain using the atomic structure code SUPERSTRUCTURE[8] and that, since it includes only spectroscopic orbitals, it is less likely to give rise to pseudoresonances at low energies. The disadvantages are that the $1s$ core orbital is optimized for the ground state and is thus not ideal for the $1s\,2l$ excited states, and that since only spectroscopic orbitals are included very little of the correlation energy of the ground state is obtained. This target is also similar in type and quality (by the usual measures) to that used in the most

TABLE IV. Target wave functions: energies and oscillator strengths.

	Total (1^1S) and excitation energies (Ry)				
Target	1^1S	1^1S-2^3S	1^1S-2^1S	1^1S-2^3P^o	1^1S-2^1P^o
1	−14.5224	4.3127	4.4472	4.4740	4.5443
2	−14.5224	4.3076	4.4472	4.4738	4.5429
3	−14.4734	4.3441	4.4760	4.5032	4.5792
vW[a]	−14.4742	4.3450	4.4884	4.5031	4.5834
Accurate[b]	−14.5598	4.3384	4.4781	4.5044	4.5731
Measured[c]		4.3371	4.4649	4.5031	4.5719

	Oscillator strengths (length, velocity)[d]		
Target	$1^1S\rightarrow2^1P^o$	$2^3S\rightarrow2^3P^o$	$2^1S\rightarrow2^1P^o$
1	0.482,0.479	0.334,0.319	0.231,0.129
2	0.466,0.463	0.319,0.383	0.240,0.165
3	0.490,0.467	0.328,0.435	0.238,0.181
vW[a]	0.525,0.510	0.342,0.411	0.211,0.162
Accurate[b]	0.457	0.308	0.213

[a]Reference 9.
[b]From the nonrelativistic multiconfiguration calculations of Ref. 10.
[c]From Ref. 11.
[d]Using measured energy differences.

accurate previous calculation for Li II.

In that work, van Wyngaarden *et al.*[9] (hereafter vW) used three Slater-type one-electron orbitals (STO) which they labeled $1s$, $2s$, and $2p$. The CI expansion for this target is also shown in Table II. This target shares the advantages and disadvantages of target 3, with the difference that like target 1, it generates no bound-channel configurations of the type $1s\,3l\,3l'$. For convenience we will refer to target 3 and the wave functions used by vW as ground-state optimized (GSO) wave functions, due to their use of the 1^1S $1s$ orbital.

In Table III we list the configuration mixing coefficients for targets 1, 2, and 3 along with those of vW. In Table IV we list the corresponding total energies, excitation energies, and oscillator strengths together with accurate values.[10,11] From the standpoint of oscillator strengths and total energies target 2 is the best, followed in order by target 1, target 3, and that of vW. If excitation energies with respect to the ground state are used as the quality criteria, then target 3 is the best, followed in order by that of vW, target 1, and target 2, very nearly the reverse of the previous ordering.

The explanation for this seeming contradiction is that in target 3 and in that of vW the error of ~ 0.086 Ry in the ground-state energy due to the neglect of correlation energy is approximately equal to the errors of ~ 0.09 Ry in the energies of the excited states due to the use of the ground-state $1s$ core orbital. When the differences are taken to arrive at the excitation energies the errors tend to cancel. Conversely, in targets 1 and 2 the errors in the total energies of the excited states are ~ 0.01 Ry or less compared to the error of ~ 0.037 Ry in the ground state due to the neglect of $\sim 43\%$ of the correlation energy. When the difference is taken the resulting excitation energies are too small.

C. Resonance effects

As noted in Sec. II B, targets 2 and 3 are specifically constructed to generate $1s\,3l3l'$ bound-channel configurations (explicit examples of the relationship between target state wave functions and the associated bound-channel configurations can be found in Pradhan *et al.*[4] and Henry[1]). A list of the lowest $1s\,3l\,3l'$ states for the first three symmetries, and their energies relative to the ground state of Li II as determined from analysis of the reactance matrices, are given in Table V for targets 2 and 3. The configuration assignments were determined by examining the eigenfunctions of the corresponding eigenvalues of $\langle \Phi \mid H \mid \Phi \rangle$. For the higher-lying states such assignments are less meaningful due to extensive CI effects.

Also shown in Table V are the positions of some $1s\,3l\,3l'$ states as determined in the quasi-projection-operator calculations of Wakid *et al.*,[12] and in measurements for the $^2P^o$ states.[13] We also give, following Mehlman *et al.*,[13] estimates of the positions of the ^2S and ^2D resonances based on calculated[14] positions of the corresponding doubly excited states of helium, and the assumption that coupling with the $1s$ core electron is weak and relatively constant. This scaling was shown[13] to be remarkably accurate, differing with the measured values by at most 0.04 Ry for the lowest few $^2P^o$ resonances. Given the relative simplicity of our models, the positions of the $^2P^o$ resonances are in quite good agreement with the measured and predicted values.

Rather than using a very large number of direct computations to delineate the detailed resonance structure in the all-channels-open region, we fit our computed R matrices to a sum of polynomial and pole terms:

$$R_{ij}(\epsilon)=\sum_{k=1}^{I_P} a_{ij}^{(k)}\epsilon^{k-1}+\sum_{n=1}^{I_Q}\frac{a_{ij}^{(I_P+n)}}{\epsilon-\epsilon_n}\ , \tag{6}$$

where the $a_{ij}^{(k)}$ are expansion coefficients, I_P is the degree of the polynomial, I_Q is the number of poles, the ϵ_n are the pole positions, and ϵ is the collision energy. Generally, five points per pole are required for a good fit.

To obtain the R matrices below the 2^1P^o threshold, including resonance structure, we use the techniques of quantum-defect theory[15] (QDT), and the very useful program RANAL,[16] which carries out the fitting and extrapolation of calculated R matrices. RANAL can also be used to average over the resonances using the theory of Gailitis.[17]

TABLE V. Resonance positions, in rydbergs, relative to the Li II ground state.

Classification[a]	Dominant configurations		Target 2	Target 3	Ref. 12	Ref. 13
$(3,3a)^1S$	^2S:	$1s3s^2$	4.822	4.827	4.794	4.852[a]
$(3,3b)^1S$		$1s3p^2+1s3d^2$	4.943	4.950	4.884	4.929[a]
$(3,3a)^3P^o$	$^2P^o$:	$1s3s3p$	4.805	4.826	4.948	4.833
$(3,3a)^1P^o$		$1s3s3p$	4.886	4.895	4.978	4.857
$(3,3b)^3P^o$		$1s3p3d$	4.988	5.003	4.994	4.948
$(3,3b)^1P^o$		$1s3p3d$	5.121	5.129	5.018	4.995
$(3,3a)^1D$	^2D:	$1s3p^2$	4.860	4.873	4.854	4.871[a]
$(3,3a)^3D$		$1s3s3d$	4.936	4.953	4.876	4.907[a]
$(3,3b)^1D$		$1s3s3d$	5.038	5.048	4.884	4.930[a]

[a]Estimated following Ref. 13, see text.

TABLE VI. Model characteristics.

	Model			
	I	II	III	IV
Target	1	1	2	3
Method	DW	CC	CC	CC

III. MODEL DESCRIPTIONS

As mentioned in the Introduction we made calculations using several different combinations of target wave functions and scattering approximations. In this section we describe the characteristics of the four models used.

In model I the DW approximation is used to obtain the contributions from the ^2S-$^2F^o$ collision symmetries. The TFD scaling factors used to generate the continuum orbitals are $\lambda_0=0.981$, $\lambda_1=0.482$, and $\lambda_{l>1}=\lambda_1$. Complete optimization based on variations of λ_l was not attempted. In models II, III, and IV the CC approximation is used to obtain the contributions from the ^2S-$^2F^o$ collision symmetries. In models I and II target 1 is used. Model III uses target 2, while model IV uses target 3. The characteristics of these four models are summarized in Table VI.

In all four models advantage is taken of the low collision energies involved, and the consequent rapid drop in the size of the contributions to the total cross sections from the higher collision symmetries, to use the DW approximation for the ^2G-$^2K^o$ collision symmetries. The contribution from these partial waves is greatest for the 2^1S and 2^1P^o cross sections, ranging from $\sim$0.5% and $\sim$2.5%, respectively, at 4.7 Ry, to $\sim$2% and $\sim$10%, respectively at 5.5 Ry. In this energy range contributions from higher partial waves are completely negligible (less than one part in 10^5 for the $^1P^o$ cross section).

Due to the presence of a large pseudoresonance near the 2^1P^o threshold in the model-I ^2S DW contribution, the program RANAL is used to obtain the nonresonant background collision strength at a point removed from the resonance. An extrapolation of this background cross section is then used instead of the directly calculated ^2S DW collision strength. While this is admittedly a somewhat *ad hoc* approach, an examination of the uncertainties in the fitting technique leads to an estimated maximum error of $\sim$20% in the ^2S DW contribution. The uncertainty in the total cross sections near threshold is thus only a few percent.

IV. RESULTS

In this section we present the cross sections obtained using our four models, and compare them with each other and with the results of vW. The collision energies have been shifted slightly ($<$0.4 eV) in the plots so that the 2^1P^o excitation threshold for each model coincides with the experimental value[11] of 4.572 Ry. (This shift was also applied to the resonance positions for targets 2 and 3 given in Table V.)

By comparing pairs of calculations we can gain some insight into the effects that target wave functions, scattering approximation, and resonance contributions can have on the cross section for each transition. Specifically,

(1) by comparing models III and IV, and model II with the results of vW, we can assess the sensitivity to target wave functions;

(2) by comparing models I and II we can assess the reli-

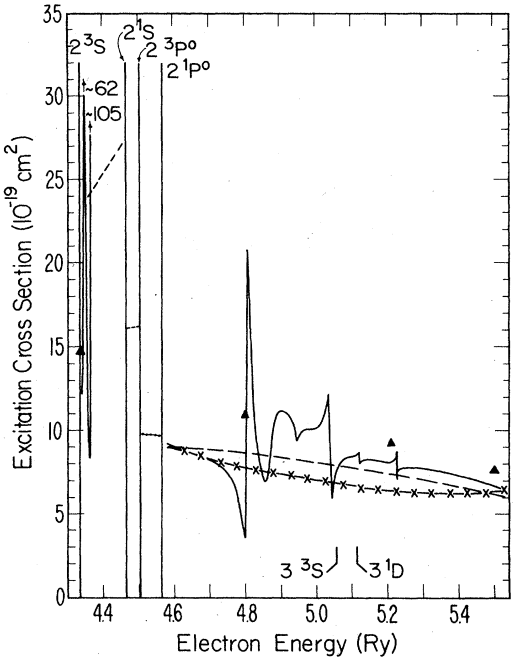

FIG. 1. $1^1S\rightarrow2^3S$ excitation cross section: -×-, model I; — — —, model II; ——, model III; - - -, numerical average over resonances, model III; —·—, Gailitis averaged resonances, model III; ▲, van Wyngaarden *et al.* (Ref. 9).

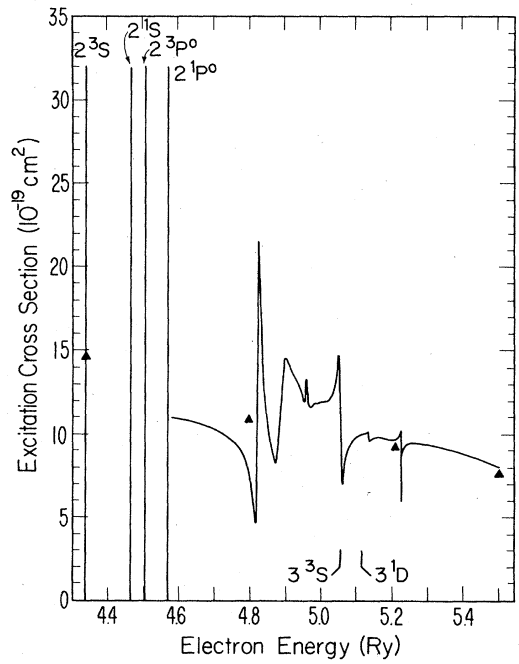

FIG. 2. $1^1S\rightarrow2^3S$ excitation cross section: ——, model IV; ▲, van Wyngaarden *et al.* (Ref. 9).

ability of the DW approximation; and

(3) by comparing models II and III we can isolate the importance of resonances in series converging on the $n=3$ levels.

A. $1^1S \rightarrow 2^3S$

Figures 1 and 2 display the calculated $1^1S \rightarrow 2^3S$ cross sections obtained using models I–IV along with the results of vW.

1. Wave-function dependence

Comparison of the results of model II with those of vW, and of model III with those of model IV, shows that the use of PC wave functions leads to a moderate reduction in the cross section relative to that obtained using GSO wave functions. The reductions are $\sim 30\%$ and $\sim 20\%$ near threshold for the first and second pairs of calculations, respectively. Although it is difficult to directly compare the vW result with that of model IV due to the presence of $1s\,3l\,3l'$ resonances in the latter, it is apparent that they yield very similar background cross sections in spite of the different origins of their one-electron radial orbitals (Hartree-Fock versus TFD).

It is interesting to note that the $1s\,3l\,3l'$ resonances evident in the model-IV results (Fig. 2) are very similar to those in the model-III results. (Minor differences resulting from differing interference between resonances are evident.) In this respect it is apparent that the source of the $3l$ orbitals (PC in model III versus TFD in model IV) is not critical to the representation of the $1s\,3l\,3l'$ states by the bound-channel configuration set. This feature is common to all four cross sections.

2. Scattering approximation dependence

From models I and II we see that the DW and CC scattering approximations yield cross sections that are very similar in magnitude in this energy range. This is quite fortuitous—there are significant (factors of 2) differences in some partial cross sections, which cancel in the total.

3. Resonance dependence

Below the 2^1P^o threshold, resonances due to autoionizing states of the type $1s\,2lnl'$ are present. In Fig. 1 we show the cross section from model III including resonance contributions from $1s\,2lnl'$ states. This cross section was obtained using the QDT techniques mentioned in Sec. II C. In the region immediately above the 2^3S threshold we show some of the detailed structure in the model-III cross section. A numerical average of the cross section over the resonances is given up to the 2^3P^o threshold, where it is replaced by the Gailitis average.

Comparing the model-II cross section with the model-III results (at the 2^1P^o threshold) we see that the effect of the $1s\,2lnl'$ resonances is to markedly increase the cross section. Between the 2^3S and 2^1S threshold the resonant cross section is ~ 3 times larger than the nonresonant background. Between the 2^1S and 2^3P^o threshold the resonant cross section is almost twice as large, while it is only $\sim 5\%$ greater between the 2^3P^o and 2^1P^o thresholds.

Comparing the cross sections from models II and III in the all-channels-open region demonstrates the effect of the $1s\,3l\,3l'$ resonances. From the 2^1P^o threshold to the first resonance, the resonant cross section is depressed relative to the nonresonant cross section. From that point to the last of the $1s\,3l\,3l'$ resonances there is a large amount of resonant structure visible in the model-III results, the net effect of which is a moderate enhancement of the resonant versus the nonresonant cross section. This pattern of an initial depression of the resonant cross section followed by an enhancement is common to all of the transitions.

B. $1^1S \rightarrow 2^1S$

Figures 3 and 4 show the $1^1S \rightarrow 2^1S$ cross sections from models I–IV and from vW.

1. Wave-function dependence

It is apparent from comparing the results of model II with those of vW, and of model III with those of model IV, that the use of PC and GSO wave functions leads to significant differences. The results of vW and model IV are $\sim 100\%$ and $\sim 65\%$ greater at threshold than those from models II and III, respectively. As is the case for the $1^1S \rightarrow 2^3S$ cross section, it is evident that the vW result is quite similar to the background of the model-IV cross section except very near threshold.

2. Scattering approximation dependence

Looking at the results of models I and II we see that cross sections from the DW and CC scattering approxi-

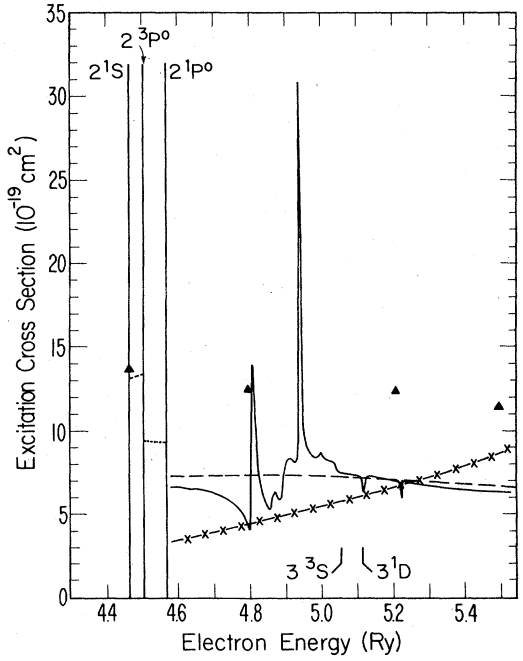

FIG. 3. $1^1S \rightarrow 2^1S$ excitation cross section: symbols as for Fig. 1.

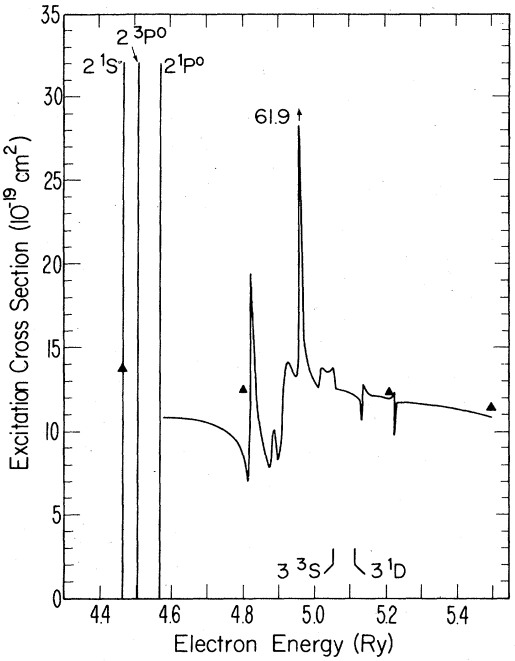

FIG. 4. $1^1S \rightarrow 2^1S$ excitation cross section: symbols as for Fig. 2.

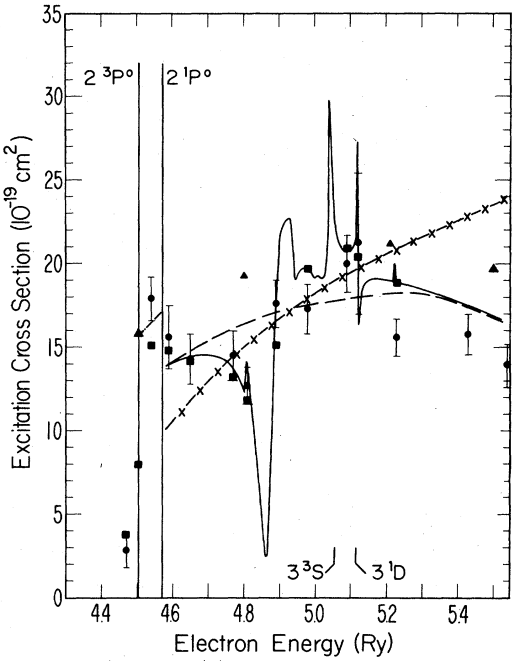

FIG. 5. $1^1S \rightarrow 2^3P^o$ excitation cross section: symbols as for Fig. 1 plus ⧫, experimental values of Rogers *et al.* (Ref. 2); ■, model-III cross section convolved with ~1-eV experimental energy resolution.

mations display very different trends with respect to energy, and differ by as much as a factor of 2.

3. *Resonance dependence*

A comparison between the nonresonant model-II cross section at the 2^1P^o threshold with the resonant model-III cross section below the threshold once again shows the enhancing effect of resonances due to $1s\,2lnl'$ autoionizing states. Between the 2^1S and 2^3P^o thresholds the resonant cross section is about twice the background, while between the 2^3P^o and 2^1P^o thresholds it is ~50% greater.

The effect of the $1s\,3l\,3l'$ autoionizing resonances in the all-channels-open region can be seen by comparing the results of model II and model III, and follows the general trend mentioned in the discussion of the $1^1S \rightarrow 2^3S$ cross section. Again, the resonance structure in model IV is quite similar to that in model III in spite of the large difference in their background cross sections.

C. $1^1S \rightarrow 2^3P^o$

The $1^1S \rightarrow 2^3P^o$ cross sections from models I–IV and from vW are shown in Figs. 5 and 6. Also shown are the absolute experimental values for the $1^1S \rightarrow 2^3P^o$ cross section obtained by Rogers *et al.*,[2] and the results of convolving the model-III cross section with their ~1-eV experimental beam width.

1. *Wave-function dependence*

Of the four transitions we examine, the $1^1S \rightarrow 2^3P^o$ transition displays the least sensitivity to whether PC or GSO wave functions are used to represent the target states. We see that the vW and model-IV results are both ~15% greater than the model-II and -III cross sections, respectively. In Fig. 6 we see again that the vW results are quite close to the model-IV background cross section.

Due to the structure visible in the experimental cross

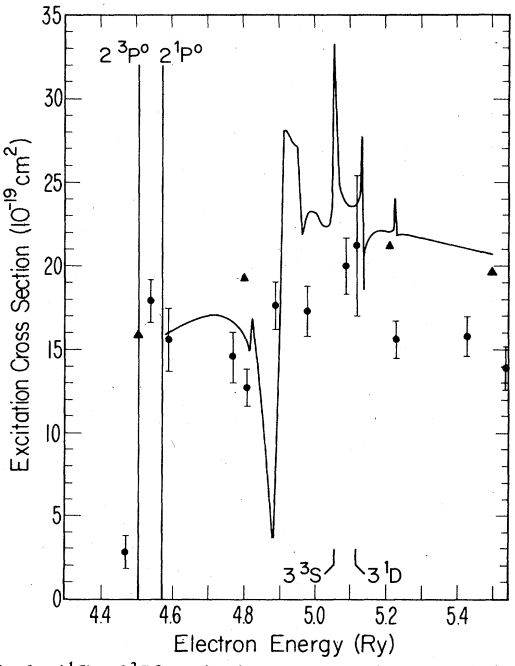

FIG. 6. $1^1S \rightarrow 2^3P^o$ excitation cross section: symbols as for Fig. 2 plus ⧫, experimental values of Rogers *et al.* (Ref. 2).

section it is not possible to uniquely differentiate between the wave-function dependence and resonance dependence of the theoretical cross sections when they are compared to the experimental values. However, it does seem safe to conclude that the CC-PC results are in better agreement with the experimental values than are the CC-GSO results.

2. *Scattering approximation dependence*

As for the $1^1S \rightarrow 2^1S$ transition, comparison of the model-I and model-II cross sections shows that the DW cross section increases more steeply with energy than the CC result. In comparing the results from models I and II with the cross section from Rogers *et al.*[2] we see that the DW approximation (model I) does a poor job of reproducing the trend of the experimental values.

3. *Resonance dependence*

The cross section from the nonresonant model-II calculation reproduces the qualitative trend of the experimental values of Rogers *et al.*[2] The resonant model-III results display not only the appropriate qualitative behavior, but, when convolved with the experimental beam width, are in good quantitative agreement with most of the experimental points below the 3^1D threshold.

The effect of the series of resonances converging on the 2^3P^o state is apparent in the measured results. The pronounced dip at 4.85 Ry is a blend of the two broadest resonances, the $(3,3a)^1P^o$ and the $(3,3a)^1D$, which apparently also have strong branching ratios to the 2^3P^o state. Also notable in our results is the absence of significant branching to the 2^3P^o state from states labeled triplets in Table V.

Above the $n=3$ thresholds the omission of flux loss to channels not included in our CC expansion may account for much of the difference between the model-III results and the measurements. It should be noted that the measured results also contain a contribution (estimated[2] to be $\sim 10\%$) from cascade from higher states that is not included in the present work.

D. $1^1S \rightarrow 2^1P^o$

The $1^1S \rightarrow 2^1P^o$ cross sections from models I–IV and from vW are shown in Figs. 7 and 8.

1. *Wave-function dependence*

This transition displays a significant dependence on the type of wave functions used. We see that the vW cross section at threshold is $\sim 60\%$ greater than the model-II result, while the model-IV cross section is $\sim 45\%$ larger than that of model III. As for the other three transitions, the vW result appears to be very close to the model-IV background cross section except quite near threshold.

2. *Scattering approximation dependence*

We see that, particularly near the 2^1P^o threshold, there is a striking difference between the model-I (DW) and model-II (CC) cross sections. They have similar slopes,

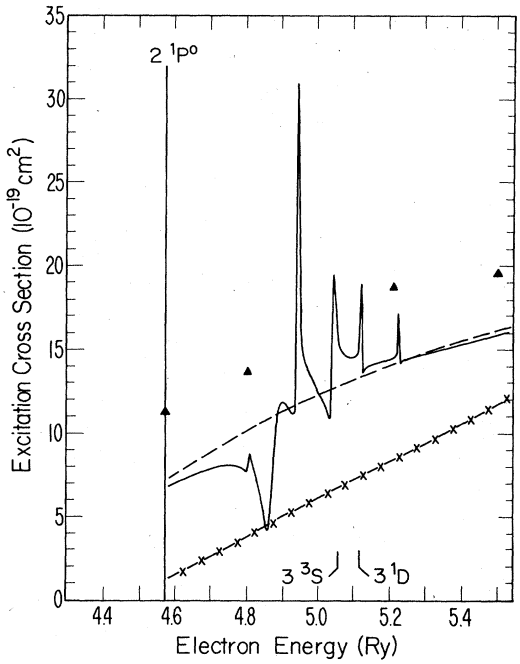

FIG. 7. $1^1S \rightarrow 2^1P^o$ excitation cross section: symbols as for Fig. 1.

but the model-I cross section is $\sim 5 \times 10^{-19}$ cm^2 less than the model-II result.

3. *Resonance dependence*

For this transition there is no contribution from autoionizing resonances of the type $1s2lnl'$. However, the $1s3l3l'$ resonances are not quite as pronounced for this

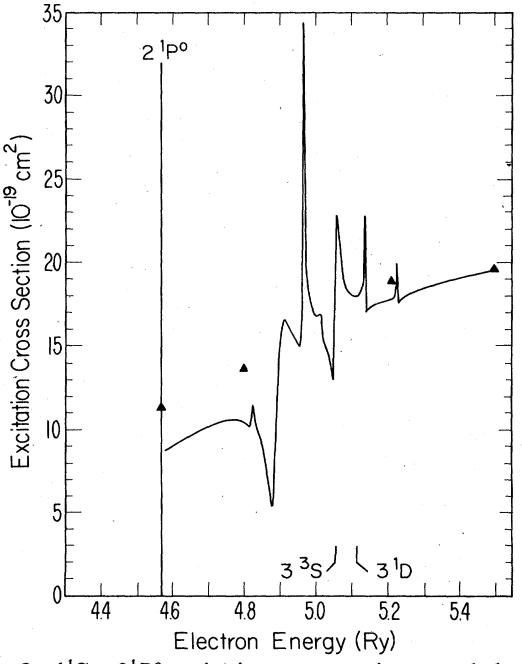

FIG. 8. $1^1S \rightarrow 2^1P^o$ excitation cross section: symbols as for Fig. 2.

dipole-allowed transition as for the spin- and dipole-forbidden transitions.

V. DISCUSSION

It comes as no surprise that the DW approximation is poor near threshold for a singly charged ion, but the differences for Li II are larger than might have been anticipated. It is also surprising that the DW approximation is markedly worse for spin-allowed than for spin-forbidden transitions, contrary to conventional wisdom.

The use of identical wave functions in our models I and II eliminates considerations of differing wave functions that have clouded some previous comparisons of DW and CC results. For example, Pradhan *et al.*[4] attributed the differences between their DW results and the CC results of vW for C V primarily to differences in target wave functions. Since the target wave functions used by Pradhan *et al.* were very similar to those of our target 3, and since there is good agreement, apart from resonance structure, between the results of our model IV and those of vW, we conclude that the differences for C V arose, in fact, primarily from the use of different scattering approximations. It should be appreciated, however, that the differences for C V are much smaller than for Li II, and confined to an energy range much nearer threshold.

The effect of resonances is quite consistent with the results and trends for higher members of helium isoelectronic sequence.[4] The 2^3S cross section is strongly affected by $n=2$ resonances, the 2^1S and 2^3P^o cross sections less so. The $n=3$ resonances, while introducing complicated structure, contribute only a modest enhancement to the cross sections in an average sense. One interesting feature of the present results is the apparent strong preferential branching of the first (second) $1s\,3s\,3p$ resonance to the $2^{3,1}S$ ($2^{3,1}P^o$) states.

Perhaps the most surprising result of our calculations is the way in which the calculated cross sections depend on the type of wave functions used to represent the target states, in particular the fact that the spin-allowed transitions are much *more* sensitive than the spin-forbidden transitions. As discussed in Sec. II B, our PC wave functions differ from our GSO wave functions (and those of vW) in two main ways: (1) the PC wave functions capture $\sim 57\%$ of the ground-state correlation energy compared to $\sim 1\%$ for the GSO wave functions; and (2) the PC wave functions allow for some of the core relaxation that occurs when one of the electrons in the ground state is excited, while the GSO wave functions do not. It is not possible, on the basis of the present results alone, to establish with certainty if, or which, one of these two differences is more responsible for the observed wave-function dependence. This and other evidence to be discussed next suggests, however, that the effect of ground-state correlation is more important for the spin-allowed than for the spin-forbidden transitions.

In their comparison of two CC calculations using different wave functions, vW found roughly equal differences near threshold for all four transitions, with the $^{3,1}P^o$ transitions being slightly more affected. The two sets of wave functions used differed primarily in the $1s$ orbital, one being hydrogenic and one being from a Hartree-Fock calculation. Thus one calculation contained more allowance for core relaxation in the excited states than the other, and the results using the former were slightly worse, but neither captured much of the ground-state correlation energy.

The other piece of evidence comes from the DW calculations of Pindzola *et al.*[18] for the 2^3P^o cross section. They used an excited-state wave function of accuracy comparable to that of our targets 1 and 2, and compared results obtained using single-configuration and multiconfiguration Hartree-Fock (MCHF) wave functions for the ground state. The MCHF wave function captured $\sim 80\%$ of the correlation energy, but differences between the calculated cross sections were small ($< 10\%$) near threshold. Thus we conclude that core relaxation affects all transitions more or less equally, and that correlation effects in the ground state are more likely to affect dipole-allowed than dipole-forbidden transitions.

We might also remark on the reliability of oscillator strengths and energy differences as guides to the relative magnitude and accuracy of results obtained using different target wave functions. Comparing the oscillator strengths for the $2^3S \rightarrow 2^3P^o$ transition in Table IV, we would (correctly) predict that the model-III (target-2) results would be the best, but be totally misled as to the relative magnitudes of the various results. Similarly, the 2^1P^o cross sections near threshold differ much more than a comparison of the oscillator strengths would suggest. Assuming that the model-III results are the best for all transitions, this is completely contrary to an assessment of wave-function quality based on excitation energies.

In conclusion we would like to make a few suggestions for future work. In view of the remarkable sensitivity of the 2^1P^o cross section to target wave functions, a measurement of this cross section would be extremely valuable. The present results may also bear on the still unresolved discrepancy between calculated[19] and measured[20] values for the $2s \rightarrow 2p$ cross section in Be^+. The discrepancy is not large ($\sim 20\%$), but very troublesome as it is several times the experimental uncertainty. Although the wave functions used in all of the calculations for Be^+ yielded good oscillator strengths and energy differences, none allowed for any effect of correlation in the $1s^2$ core of the target.

ACKNOWLEDGMENTS

This work was supported by the U.S. Department of Energy (Office of Basic Energy Sciences), and by a grant of computer time from the U.S. National Center for Atmospheric Research.

*Present address: L-35, Lawrence Livermore National Laboratory, Livermore, CA 94550.
†Quantum Physics Division, National Bureau of Standards.

[1]R. J. W. Henry, Phys. Rep. **68**, 1 (1981).
[2]W. T. Rogers, J. O. Olsen, and G. H. Dunn, Phys. Rev. A **18**, 1353 (1978).
[3]M. A. Hayes and M. J. Seaton, J. Phys. B **11**, L79 (1978).
[4]A. K. Pradhan, D. W. Norcross, and D. G. Hummer, Phys. Rev. A **23**, 619 (1981).
[5]W. Eissner and M. J. Seaton, J. Phys. B **5**, 2187 (1972).
[6]M. A. Crees, M. J. Seaton, and P. M. H. Wilson, Comput. Phys. Commun. **15**, 23 (1978).
[7]M. J. Seaton and P. M. H. Wilson, J. Phys. B **5**, L175 (1972).
[8]W. Eissner and H. Nussbaumer, J. Phys. B **2**, 1028 (1969).
[9]W. L. van Wyngaarden, K. Bhadra, and R. J. W. Henry, Phys. Rev. A **20**, 1409 (1979); and private communication.
[10]A. W. Weiss, J. Res. Natl. Bur. Stand. Sect. A **71**, 163 (1967).
[11]C. E. Moore, *Atomic Energy Levels,* Natl. Bur. Stand. (U.S.) Circ. No. 467 (U.S. GPO, Washington, D.C., 1949).
[12]S. Wakid, A. K. Bhatia, and A. Temkin, Phys. Rev. A **21**, 496 (1980).
[13]G. Mehlman, J. W. Cooper, and E. B. Saloman, Phys. Rev. A **25**, 2113 (1982).
[14]L. Lipsky, R. Anania, and M. J. Conneely, At. Data Nucl. Data Tables **20**, 127 (1977).
[15]M. J. Seaton, Rep. Prog. Phys. **46**, 167 (1983); and references therein.
[16]A. K. Pradhan and M. J. Seaton (private communication).
[17]M. Gailitis, Zh. Eksp. Teor. Fiz. **44**, 1753 (1963) [Sov. Phys.—JETP **17**, 1328 (1963)].
[18]M. S. Pindzola, A. K. Bhatia, and A. Temkin, Phys. Rev. A **22**, 132 (1980).
[19]M. A. Hayes, D. W. Norcross, J. B. Mann, and W. D. Robb, J. Phys. B **10**, L429 (1977); R. J. W. Henry and W. L. van Wyngaarden, Phys. Rev. A **17**, 798 (1978).
[20]P. O. Taylor, R. A. Phaneuf, and G. H. Dunn, Phys. Rev. A **22**, 435 (1980).